

Threshold devices: Fractal noise and neural talk

Peter Jung

*University of Illinois at Urbana-Champaign, Center for Complex Systems Research, Beckman Institute,
405 North Mathews Avenue, Urbana, Illinois 61801*

(Received 31 March 1994)

We consider the statistical properties of random pulse trains generated by noisy signals imposed on a threshold device—a simple model for the information processing of a single neuron. It is shown that Markovian noise generates self-similar bursts characterized by algebraic decaying correlations and power spectra. It is further shown that the role of noise is ambiguous. For subthreshold signals, noise can enhance the performance of the threshold device, whereas above threshold noise always degrades a signal.

PACS number(s): 05.40.+j

I. INTRODUCTION

The human brain, the most powerful signal processing tool we know, operates via firing pulses between neurons, triggered by external or internal stimuli. Although the dynamics of a neuron is far too complex to be described by a few dynamical equations it is hoped that some characteristic features can be captured in tractable models. The most common model to simulate the spiking behavior of a simple neuron has been put forward by Hodgkin and Huxley, Fitzhugh, and Nagumo (HHFN) and others [1]. It is in its simplest form a two-dimensional dynamical system. In view of applications to the statistical mechanics of neural networks with a large number of neurons, one wishes to have more simple models for the single neuron than HHFN. McCulloch and Pitts [2] have introduced an extremely simple model which allows the model neuron to be in two states, a nonactivated quiescent state and a firing state. When the voltage across the membrane of the neuron is below threshold, the model neuron is in the quiescent state (Q). When the membrane voltage crosses threshold, the model neuron switches to the firing state (F), i.e., it fires a pulse, and is subsequently reset within a certain refractory period to its nonactivated quiescent state. Within this model, the output of the neuron can be described as a binary sequence of states (Q) and (F), or equivalently as a binary pulse train. Many neurons (depending on the function of the neuro-group they belong to) are intrinsically very noisy, thus showing spontaneous firing activity, even without an external stimulus. The outgoing pulse train is to be considered a random pulse train even in the presence of a stimulus. Both the external stimulus and the noise trigger the pulse train (the output of the neuron) in a possibly cooperative fashion. In a recent experiment with periodically stimulated mechanoreceptor cells of crayfishes [3], the spectral properties of the pulse trains of real neurons have been studied. Synergetic effects of noise and stimulus have been observed for the signal transfer. It is actually improved by a certain amount of noise in the neuron. Similar observations in non-neuronal systems have been made in [4].

These remarkable results have stimulated the research

presented in this paper. In a recent paper [5] by Bulsara and Lowen, the escape time distribution of a linear integrate-and-fire model with white noise and periodic perturbation has been studied. Every escape event prompts a sharp pulse and the spectral density of the generated pulse train has been evaluated. It is important to note in the context of the results in the present paper that in [5] an explicit dephasing has been used, i.e., the phase of the periodic perturbation has been reset at every escape event. This destroys the long-time coherence one would observe otherwise, but allows one to use the well established mathematical apparatus for renewal processes (see, e.g., in [6]). The goal of this paper, complementary to [5], is to study the pulse trains, generated by *threshold crossing* events without resetting phases and therefore without neglecting correlations between different pulses. Similar work, but for different pulse shapes, is in progress by Gingl, Kiss, and Moss [7]. Although barrier crossing and first passage time distributions have been studied intensively in the past and are understood well (for a review, see [8]), the theory of noise induced *threshold crossing* is developed only fragmentarily.

The preceding paragraph already roughly outlines this paper. Although the motivation for this work is neural dynamics, we address here the problems of threshold crossing, pulse generation, and spectral properties of pulse trains from a more general viewpoint based on models which are not always close to the neural reality. In Sec. II we introduce two noise sources which are different with respect to their smoothness, an important issue for threshold-crossing statistics and for the spectral properties of the pulse train. We are using a single low-pass filtered white noise (SL) and a double low-pass filtered white noise (DL) as sources for fluctuations. The latter is non-Markovian while the former is Markovian with an unbound variation of the derivative. Results in this paper show that the number of derivatives with bounded variation actually provides the classification scheme for the smoothness with respect to the spectral properties of the generated pulse train. We briefly describe concepts for threshold-crossing rates in the presence of noise only (see, for instance, [9,10]). In Sec. III we will turn to spectral properties of pulse trains, gen-

erated by the threshold element by firing a pulse whenever the fluctuation passes a certain threshold. These sorts of random processes have been termed triggered processes. The θ trigger describes a pulse train which is zero when the noise level at the input of the threshold element is below a threshold and one if it is above. We derive explicit equations for the correlation function and the spectral density. In Sec. IV we use the groundwork, laid out in Sec. III to extend our considerations to threshold elements driven by noise and external periodic signals. We will discuss the correlation of the random pulse trains with the stimulus as a measure for the signal-processing performance of the threshold element. We do not restrict ourselves to small signals, small frequencies of the stimulus, or to correlation-free events.

II. THRESHOLD-CROSSING RATES OF STATIONARY RANDOM PROCESSES

In this section we briefly review threshold-crossing rates for smooth random processes. The precise meaning of smooth is developed in this section. For nonsmooth processes a threshold-crossing rate, strictly spoken, does not exist. Nevertheless some concepts can be generalized to yield answers also for Markovian systems.

A. Smooth random processes

Consider a stationary random process $x(t)$, described by the probability density $p_2(x, \dot{x})$, where \dot{x} is the time derivative of $x(t)$. Assuming the derivative \dot{x} being a random process of finite variation within the interval $(t, t+dt)$, the probability that the random variable crosses the threshold b in the interval $(t, t+dt)$ is then given by $dW = p_2(b, \dot{x}) d\dot{x} \dot{x} dt$. The mean threshold-crossing rate for crossing from below threshold to above threshold is thus given by [10,9]

$$\alpha = \int_0^\infty p_2(b, \dot{x}) \dot{x} d\dot{x} . \quad (1)$$

For a Gaussian process with the stationary probability density

$$p_2(x, \dot{x}) = \frac{1}{2\pi\sqrt{\sigma_{xx}\sigma_{\dot{x}\dot{x}}}} \exp\left[-\frac{x^2}{2\sigma_{xx}} - \frac{\dot{x}^2}{2\sigma_{\dot{x}\dot{x}}}\right], \quad (2)$$

$$\sigma_{\dot{x}\dot{x}} = -\frac{d^2}{dt^2} \langle x(t)x(0) \rangle|_{t=0} \equiv -K''(0),$$

and σ_{xx} being the variance $\langle x^2 \rangle$, the threshold-crossing rate (1) is given by [10]

$$\alpha = \frac{1}{2\pi} \left[-\frac{K''(0)}{K(0)} \right]^{1/2} \exp\left[-\frac{b^2}{2K(0)}\right]. \quad (3)$$

Expressing the stationary correlation function $K(t) = \langle x(t)x(0) \rangle$ by the spectral density $S(\omega)$ by using Wiener-Khinchines theorem, i.e.,

$$S(\omega) = \int_{-\infty}^{\infty} K(t) \exp(-i\omega t) dt, \quad (4)$$

we obtain the following expression for the threshold-crossing rate [9]:

$$\alpha = \frac{1}{2\pi} \left[\frac{\int_{-\infty}^{\infty} S(\omega) \omega^2 d\omega}{\int_{-\infty}^{\infty} S(\omega) d\omega} \right]^{1/2} \exp\left[-\frac{\pi b^2}{\int_{-\infty}^{\infty} S(\omega) d\omega}\right]. \quad (5)$$

The smoothness condition can now be specified more precisely: the spectral density has to decay for large frequencies proportional to $\omega^{-\kappa}$ with $\kappa \geq 4$. In particular, for Markovian processes where the spectral densities decay proportional to ω^{-2} , the threshold-crossing rate is infinite.

In this paper, we make use of two random processes for generating pulse trains, a single low-pass filtered white noise process $x(t)$ (SL), described by

$$\dot{x}(t) = -\frac{1}{\tau_1} x + \frac{\sqrt{D}}{\tau_1} \xi(t), \quad (6)$$

with $\xi(t)$ being Gaussian white noise with zero mean and $\langle \xi(t)\xi(t') \rangle = 2\delta(t-t')$, and a double low-pass filtered white noise process $y(t)$ (DL), generated by

$$\begin{aligned} \dot{y} &= -\frac{1}{\tau_2} y + \frac{1}{\tau_2} x, \\ \dot{x} &= -\frac{1}{\tau_1} x + \frac{\sqrt{D}}{\tau_1} \xi(t). \end{aligned} \quad (7)$$

The stationary correlation function and the spectral density of SL are given by

$$K_1(t) \equiv \langle x(t)x(0) \rangle = \frac{D}{\tau_1} \exp\left[-\frac{t}{\tau_1}\right] \quad (8)$$

and

$$S_1(\omega) = \frac{2D}{1 + \omega^2 \tau_1^2}, \quad (9)$$

respectively. The stationary correlation function and spectral density of DL are given by

$$\begin{aligned} K_2(t) \equiv \langle y(t)y(0) \rangle &= \frac{D\tau_2}{\tau_2^2 - \tau_1^2} \exp\left[-\frac{t}{\tau_2}\right] \\ &\quad - \frac{D\tau_1}{\tau_2^2 - \tau_1^2} \exp\left[-\frac{t}{\tau_1}\right] \end{aligned} \quad (10)$$

and

$$S_2(\omega) = \frac{2D}{(\tau_1\tau_2\omega^2 - 1)^2 + (\tau_1 + \tau_2)^2\omega^2}, \quad (11)$$

respectively. In the limit $\tau_2 \rightarrow 0$, the spectral density $S_2(\omega)$ of DL approaches that of SL. With $K_2''(0)/K_2(0) = -1/(\tau_1\tau_2)$, the threshold-crossing rate (3) is then obtained as

$$\alpha = \frac{1}{2\pi\sqrt{\tau_1\tau_2}} \exp\left[-\frac{b^2}{2D(\tau_1 + \tau_2)}\right]. \quad (12)$$

Taking the limit $\tau_2 \rightarrow 0$, i.e., approaching a Markovian process, the threshold-crossing rate diverges as expected from the more general considerations above.

It is interesting to note that the key equation (1) can be obtained in the particular situation of a two-dimensional pair process, such as (7), by analyzing the mean probability flux across $y = b$. The Fokker-Planck equation for the joint probability distribution function $p_2(y, \dot{y}, t)$, given by

$$\begin{aligned} \frac{\partial}{\partial t} p_2(y, \dot{y}, t) = & \left[-\frac{\partial}{\partial y} \dot{y} + \left(\frac{1}{\tau_1} + \frac{1}{\tau_2} \right) \frac{\partial}{\partial \dot{y}} \dot{y} + \frac{1}{\tau_1 \tau_2} \frac{\partial}{\partial \dot{y}} y \right. \\ & \left. + \frac{D}{\tau_1^2 \tau_2^2} \frac{\partial^2}{\partial \dot{y}^2} \right] p_2(y, \dot{y}, t) \\ \equiv & \mathbf{L}_2 p_2(y, \dot{y}, t), \end{aligned} \quad (13)$$

yields for the total, stationary outgoing flux across $y = b$

$$S_y^{\text{tot}} = \int_0^\infty \dot{y} p_2(y, \dot{y}) d\dot{y}, \quad (14)$$

in agreement with the threshold-crossing rate (1).

B. Markovian processes

The threshold-crossing rate of a Markovian process diverges as shown in the preceding section. This is due to the unbound variation of the derivative of a Markovian process. In other words, there are an infinite number of crossings within any interval of time $(t, t + dt)$. It can be shown, however [10], that the density of crossings is not homogeneous, but rather shows well separated clusters of crossings. It has been argued in [10] that the mean time interval between two consecutive clusters is given for weak noise by the mean first passage time T_{MF} to reach the threshold. In particular, for our single low-pass filtered white noise process (6), one obtains for weak noise, i.e., $D \ll \tau_1 b^2$ [10],

$$\alpha_c = \frac{1}{\tau_1} \left[\frac{b^2}{2\pi\sigma} \right]^{1/2} \exp \left[-\frac{b^2}{2\sigma} \right], \quad (15)$$

with $\sigma = D/\tau_1$. The same expression up to a factor of 2 holds for the escape rate of an overdamped particle over a cusp-shaped barrier [11]. To obtain (15) one has to evaluate the steady-state nonequilibrium solution of the Fokker-Planck equation with an absorbing boundary at $x = b$ and a reinjection after x has crossed the threshold b .

Closer to the notation of threshold crossing is the concept of flux across a threshold. In the case of the double low-pass filtered white noise process, this concept yields the same answer as the one by Rice and Stratonovich presented above. Important for the flux-over-threshold concept to apply is the existence of a steady-state current, which requires nonpotential conditions. The single low-pass filtered white noise, as a Markovian one-dimensional process, has no nonvanishing stationary current—the forward and the backward flux balance each other—and the flux-over-threshold method is not applicable immediately. Nevertheless, by adopting the cutting principle of classical mechanics, we are able to find the forward and the backward flux separately. Consider the single low-pass filtered white noise; the stationary probability density is given by

$$p_1(x) = \frac{1}{\sqrt{2\pi\sigma}} \exp \left[-\frac{x^2}{2\sigma} \right]. \quad (16)$$

At time $t = t_0$, we cut our system into two subsystems (U_1) and (U_2),

$$x \in \begin{cases} U_1 & \text{if } x < b \\ U_2 & \text{if } x > b. \end{cases} \quad (17)$$

Both subsystems are connected due to the forward and backward flux S_+ and S_- across $x = b$, respectively. To find S_+ , we separate the subsystems from each other and calculate the momentary flux out of U_1 , i.e.,

$$\begin{aligned} S_+(x, t = t_0) = & -\frac{1}{\tau_1} \Theta(b-x) p_1(x) x \\ & - \frac{D}{\tau_1^2} \frac{\partial}{\partial x} \Theta(b-x) p_1(x) \\ = & \frac{D}{\tau_1^2} \delta(b-x) p_1(b) \\ = & \frac{1}{\tau_1} \left[\frac{\sigma}{2\pi} \right]^{1/2} \exp \left[-\frac{b^2}{2\sigma} \right] \delta(b-x). \end{aligned} \quad (18)$$

The flux $S_-(x, t = t_0)$ is obtained in the same way and is just the negative of $S_+(x, t = t_0)$. In contrast to the cluster-repetition rate (15), the forward flux (18) has a different prefactor and is valid for all values of the noise variances σ . It is also important to note that the forward current S_+ for the Markovian system (SL) as well as the threshold-crossing rate α of the double low-pass filtered white noise are monotonous increasing functions of the respective variances.

III. TRIGGERED PROCESSES

The type of triggered process we consider in this paper is a sequence of pulses at times where a continuous random process $y(t)$ crosses a certain threshold. The pulse train takes on the values $s(t) = s_0$, if the random process $y(t)$ is larger than the threshold b and is otherwise zero, i.e.,

$$s_\Theta(t) = s_0 \Theta(y(t) - b) = \begin{cases} 0 & \text{for } y(t) < b \\ s_0 & \text{for } y(t) > b. \end{cases} \quad (19)$$

We are interested in the probability density, correlation functions, and spectral densities of the generated random pulse trains.

A. The probability density

The pulse generating processes we consider are the single low-pass filtered white noise process $x(t)$, (6), and the double low-pass filtered process $y(t)$, (7). It is described by the Fokker-Planck equation (13) with the stationary density

$$p_2(y, \dot{y}) = \frac{1}{2\pi\sqrt{\sigma_{yy}\sigma_{\dot{y}\dot{y}}}} \exp \left[-\frac{\dot{y}^2}{2\sigma_{\dot{y}\dot{y}}} - \frac{y^2}{2\sigma_{yy}} \right], \quad (20)$$

with

$$\begin{aligned}\sigma_{yy} &= \frac{D}{\tau_1 + \tau_2}, \\ \sigma_{\dot{y}\dot{y}} &= \frac{D}{\tau_1 \tau_2 (\tau_1 + \tau_2)}.\end{aligned}\quad (21)$$

The stationary mean value of the random pulse train is given by

$$\begin{aligned}\langle s_\Theta \rangle &= s_0 \int_{-\infty}^{\infty} dy \int_{-\infty}^{\infty} d\dot{y} \Theta(y-b) p_2(y, \dot{y}) \\ &= \frac{s_0}{2} \operatorname{erfc} \left[\frac{b}{\sqrt{2\sigma_{yy}}} \right],\end{aligned}\quad (22)$$

with $\operatorname{erfc}(x)$ being the complementary error function. The stationary probability density of the random pulse train is nonzero only for $s=0$ and s_0 , i.e.,

$$p_{st}(s) = p_0 \delta(s) + p_1 \delta(s - s_0), \quad (23)$$

where

$$\begin{aligned}p_0 &= 1 - \langle s_\Theta \rangle, \\ p_1 &= \langle s_\Theta \rangle.\end{aligned}\quad (24)$$

It is interesting to note here that the probability for the state $s=s_0$ is not of Boltzmann type as it is usually assumed in the statistical mechanics of neuronal networks (see, for instance, [12]). The canonical distribution in those theories is based on the analogy of a statistical spin system with the two-state neuron and the assumption of *thermodynamic equilibrium*. In our stochastic model, the pulse generating fluctuations are equilibrium fluctuations. This, however, does not imply that the pulse equilibrates in time, since the pulse cannot dissipate into a heat bath.

For small variances i.e., $\sigma_{yy} \ll b^2$, the probability $p_1(t)$ is given by

$$p_1 \approx s_0 \left(\frac{2\sigma_{yy}}{b\pi^2} \right)^{1/2} \exp \left[-\frac{b^2}{2\sigma_{yy}} \right], \quad (25)$$

whereas for large variances, i.e., $\sigma_{yy} \gg b^2$, the probability saturates,

$$\begin{aligned}C_{\text{SL}}(t) &\equiv \langle s_\Theta(t) s_\Theta(0) \rangle - \langle s_\Theta \rangle^2 \\ &= \int_b^\infty dx \int_b^\infty dx' P(x, t | x', 0) p_1(x') - \langle s_\Theta \rangle^2 \\ &= \frac{s_0^2}{2} \frac{1}{\sqrt{2\pi\sigma}} \int_b^\infty dx \exp \left[-\frac{x^2}{2\sigma} \right] \operatorname{erfc} \left[\frac{b-x \exp(-t/\tau_1)}{\sqrt{2\sigma(t)}} \right] - \langle s_\Theta \rangle^2,\end{aligned}\quad (32)$$

with $\sigma \equiv \sigma(\infty)$. In order to evaluate the integral (32) asymptotically for small times, we use $\operatorname{erfc}(-x) = 2 - \operatorname{erfc}(x)$ and substitute $x \exp(-t/\tau_1)$ and $\sigma(t)$ by x' and $2Dt/\tau_1^2$, respectively, yielding

$$\begin{aligned}C_{\text{SL}}(t) &\approx C_{\text{SL}}(0) - \frac{1}{2} \left[\frac{1}{2\pi\sigma} \right]^{1/2} \int_b^\infty dx \exp \left[-\frac{x^2}{2\sigma} \right] \\ &\quad \times \operatorname{erfc} \left[\frac{x-b}{4Dt/\tau_1} \right].\end{aligned}\quad (33)$$

$$p_1 \approx \frac{1}{2} s_0 \left[1 - \frac{2b}{\sqrt{2\pi\sigma_{yy}}} \right]. \quad (26)$$

B. Correlation functions and spectral densities

The spectral properties of the random pulse train are contained in its autocorrelation function, given by

$$\begin{aligned}C(t) &= \langle s_\Theta(t) s_\Theta(0) \rangle - \langle s_\Theta \rangle^2 \\ &= s_0^2 \int_b^\infty dy \int_b^\infty dy' \int_{-\infty}^\infty d\dot{y} \int_{-\infty}^\infty d\dot{y}' p_2(y', \dot{y}') \\ &\quad \times P(y, \dot{y}, t | y', \dot{y}', 0) - \langle s_\Theta \rangle^2,\end{aligned}\quad (27)$$

where $P(y, \dot{y}, t | y', \dot{y}', 0)$ is the transition probability density and $p_2(y, \dot{y})$ the stationary joint probability density. For $t=0$, the correlation function is given by

$$\begin{aligned}C(t=0) &= s_0^2 \int_b^\infty dy \int_{-\infty}^\infty d\dot{y} p_2(y, \dot{y}) - \langle s_\Theta \rangle^2 \\ &= s_0 \langle s_\Theta \rangle - \langle s_\Theta \rangle^2,\end{aligned}\quad (28)$$

whereas for large times t we find

$$\begin{aligned}C(t \rightarrow \infty) &= s_0^2 \left[\int_b^\infty dy \int_{-\infty}^\infty d\dot{y} p_2(y, \dot{y}) \right]^2 - \langle s_\Theta \rangle^2 \\ &= 0.\end{aligned}\quad (29)$$

For further calculations we consider SL and DL separately.

1. Correlation function and spectral density of SL

The transition probability density is given by

$$P(x, t | x', 0) = \frac{1}{\sqrt{2\pi\sigma(t)}} \exp \left[-\frac{[x - x' \exp(-t/\tau_1)]^2}{2\sigma(t)} \right], \quad (30)$$

with

$$\sigma(t) = \frac{D}{\tau_1} [1 - \exp(-2t/\tau_1)]. \quad (31)$$

The correlation function of the pulse train can then be written as a single integral

Within a saddle point approximation, the integral in (33) is evaluated in leading order of t as

$$C_{\text{SL}}(t) \approx C_{\text{SL}}(0) - \frac{1}{\pi\sqrt{2}} \exp \left[-\frac{b^2}{2\sigma} \right] \left[\frac{t}{\tau_1} \right]^{1/2}. \quad (34)$$

The correlation function thus decays algebraically for small times. In Fig. 1 we show the numerically evaluated correlation function (32). For small times, one can actually observe the turnover from algebraic decay for small times to exponential decay for large times.

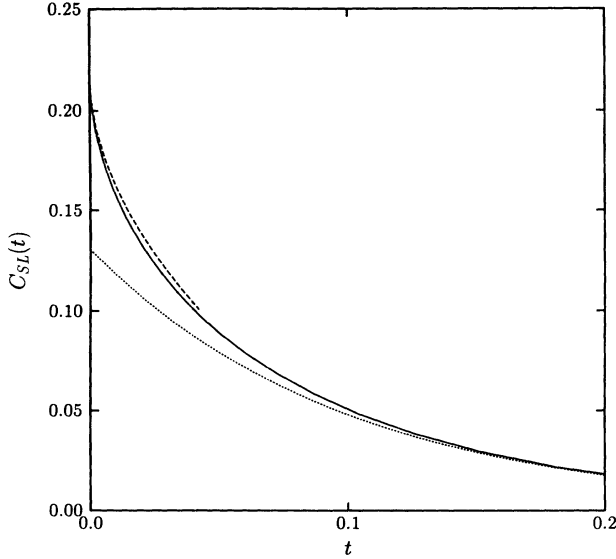


FIG. 1. The correlation function $C_{SL}(t)$ is shown for $b=1$, $d=0.5$, and $\tau_1=1$. The long-dashed line represents the short-time approximation (34) and the dotted line shows the long-time approach (36). The solid lines show the numerical integration of (32).

The large time behavior can be obtained by inserting the spectral representation of the transition probability density into (32) (see the Appendix). For the derivative of the correlation function, we can actually find a closed form, i.e.,

$$\frac{d}{dt} C_{SL}(t) = -\frac{1}{2\pi} \exp\left[-\frac{b^2}{2\sigma}\right] \frac{\exp(-t/\tau_1)}{\sqrt{1-\exp(-2t/\tau_1)}} \times \exp\left[-\frac{b^2}{2\sigma} \frac{[1-\exp(-t/\tau_1)]^2}{1-\exp(-2t/\tau_1)}\right]. \quad (35)$$

For small times we reobtain the algebraic decay (34), whereas for large times we identify exponential decay, i.e.,

$$C_{SL}(t)_{t \rightarrow \infty} \approx \frac{1}{2\pi} \exp\left[-\frac{b^2}{\sigma}\right] \exp(-t/\tau_1). \quad (36)$$

Note that the Arrhenius factor in the large time limit differs from that in the small time limit by a factor of 2. The different behavior of the correlation function for large times and for small times implies a splitting in two different correlation functions, a short-time correlation function and a large time correlation function. The

short-time correlation function describes the self-correlation within one pulse, i.e., when the random process $x(t)$ has not yet recrossed to $x < b$. The large time correlation function describes the correlation between two different pulses. Accordingly, the occurrence of a pulse at time t is not independent of the prehistory as is usually assumed for shot noise processes. The assumption of a Poisson statistics is only justified when the pair-correlation function is small. By virtue of (36) this limit can be identified at the weak noise limit.

Algebraic decay of correlation functions for small times affects the spectral density at large frequencies. The analytic continuation of the small time approximation (34), i.e.,

$$C_{SL}(t) \approx C_{SL}(0)(1-\sqrt{\beta t}) \approx C_{SL}(0)\exp(-\sqrt{\beta t}), \quad (37)$$

with

$$\beta = \frac{1}{2\pi^2} \frac{\exp(-b^2/\sigma)}{\tau_1 C_{SL}^2(0)}, \quad (38)$$

can be Fourier transformed, yielding an expression containing Fresnel functions. Expanding the Fresnel functions [13] for large frequencies ω , the asymptotic spectral density is then obtained as

$$S_{as}(\omega \rightarrow \infty) = \left[\frac{\beta}{2\omega^3 \pi} \right]^{1/2}, \quad (39)$$

i.e., it shows algebraic decay.

Algebraic decay of a correlation indicates the lack of a time scale which is an important ingredient for self-similarity. Noise which shows such correlation has been termed fractal noise [6]. This can be interpreted in the following way: A Markovian process has an infinite fine structure which cannot be resolved, e.g., with a computer. On a certain resolution, we would observe a pulse train with Θ pulses (p_1) of finite width. Increasing the resolution, i.e., looking at smaller time scales, we would find another sequence of Θ pulses (p_2), where the pulses have a smaller width. Stretching the time scale, however, reveals a pulse train being in the same sample space as (p_1). The pulse trains on both time scales are statistically self-similar. This process can be continued ad infinitum, giving rise to bursts which lack a time scale, manifest by algebraic decay of correlations.

2. Correlation functions and spectral density of DL

For the double low-pass filtered process, the transition probability density is given by (see, for instance, [14])

$$P(y, \dot{y}, t | y', \dot{y}', 0) = \frac{1}{2\pi \sqrt{\det(\underline{g})}} \exp\left\{-\frac{[y - y_t(y', \dot{y}')]^2}{2\sigma_{yy}(t)/\det(\underline{g})}\right\} \exp\left\{-\frac{[\dot{y} - \dot{y}_t(y', \dot{y}')]^2}{2\sigma_{\dot{y}\dot{y}}(t)/\det(\underline{g})}\right\} \exp\left\{-\frac{[y - y_t(y', \dot{y}')] [\dot{y} - \dot{y}_t(y', \dot{y}')] }{\sigma_{y\dot{y}}(t)/\det(\underline{g})}\right\}, \quad (40)$$

with

$$y_t(y, \dot{y}) = A(y, \dot{y}) \exp(-t/\tau_1) + B(y, \dot{y}) \exp(-t/\tau_2),$$

$$A(y, \dot{y}) = \frac{\tau_1 \tau_2}{\tau_1 - \tau_2} \left[\dot{y} + \frac{y}{\tau_2} \right], \quad (41)$$

$$B(y, \dot{y}) = -\frac{\tau_1 \tau_2}{\tau_1 - \tau_2} \left[\dot{y} + \frac{y}{\tau_1} \right],$$

and

$$\sigma_{yy}(t) = \frac{D}{(\tau_1 - \tau_2)^2} \left[\tau_1 + \tau_2 + \frac{4\tau_1 \tau_2}{\tau_1 + \tau_2} \left\{ \exp \left[-\left[\frac{1}{\tau_1} + \frac{1}{\tau_2} \right] t \right] - 1 \right\} - \tau_1 \exp \left[-\frac{2}{\tau_1} t \right] - \tau_2 \exp \left[-\frac{2}{\tau_2} t \right] \right],$$

$$\sigma_{\dot{y}\dot{y}}(t) = \frac{D}{(\tau_1 - \tau_2)^2} \left[\frac{1}{\tau_1} + \frac{1}{\tau_2} + \frac{4}{\tau_1 + \tau_2} \left\{ \exp \left[-\left[\frac{1}{\tau_1} + \frac{1}{\tau_2} \right] t \right] - 1 \right\} - \frac{1}{\tau_1} \exp \left[-\frac{2}{\tau_1} t \right] - \frac{1}{\tau_2} \exp \left[-\frac{2}{\tau_2} t \right] \right], \quad (42)$$

$$\sigma_{y\dot{y}}(t) = \frac{D}{(\tau_1 - \tau_2)^2} \left[\exp \left[-\frac{1}{\tau_1} t \right] - \exp \left[-\frac{1}{\tau_2} t \right] \right],$$

$$\det(\underline{\sigma}) = \sigma_{yy}(t) \sigma_{\dot{y}\dot{y}}(t) - \sigma_{y\dot{y}}^2(t).$$

Inserting (40) into (32), the integrations in (32) can be carried through up to a double integral, i.e.,

$$C_{DL}(t) = \langle s_{\Theta}(t) s_{\Theta}(0) \rangle - \langle s_{\Theta} \rangle^2$$

$$= C_{DL}(0) - \frac{s_0^2}{4\pi \sqrt{\sigma_{yy} \sigma_{\dot{y}\dot{y}}}} \int_b^{\infty} dy \int_{-\infty}^{\infty} d\dot{y} \exp \left[-\frac{y^2}{2\sigma_{yy}} - \frac{\dot{y}^2}{2\sigma_{\dot{y}\dot{y}}} \right] \operatorname{erfc} \left\{ \frac{y_t(y, \dot{y}) - b}{\sqrt{2\sigma_{yy}(t)}} \right\}. \quad (43)$$

In leading order in time t , y_t can be substituted by $y + \dot{y}t$ and the integrations can be carried through within saddle point approximation, yielding

$$C_{DL}(t) \approx C_{DL}(0) - \frac{1}{2\pi \sqrt{\tau_1 \tau_2}} \exp \left[-\frac{b^2}{2\sigma_{yy}} \right] t$$

$$= C_{DL}(0) - \alpha t, \quad (44)$$

with the threshold-crossing rate α (12). The decay of the correlation is in contrast to the case with the single low-pass filtered white noise process, not algebraic. The additional low-pass filtering with the time constant τ_2 has destroyed the fractal property of the pulse train. As a consequence, the self-similar bursting of the pulse train has disappeared (see Fig. 2). The spectral density for large frequencies decays accordingly proportional to ω^{-2} . Furthermore, it is a remarkable result that the derivative of the pulse-correlation function is given by the negative threshold-crossing rate. In the limit of the single low-pass filtered white noise, the threshold-crossing rate as well as the slope of the correlation function are infinite.

For large times, the correlation function can be evaluated by using the spectral representation of the transition probability density in terms of the eigenfunctions and eigenvalues of the Fokker-Planck operator in (13). The eigenvalues of L_2 ,

$$L_2 \psi_{mn} = -\lambda_{mn} \psi_{mn}, \quad (45)$$

are given by

$$\lambda_{mn} = n \frac{1}{\tau_1} + m \frac{1}{\tau_2}, \quad (46)$$

whereas the eigenfunctions have to be constructed iteratively. Assuming $\tau_2 \ll \tau_1$, the eigenvalue λ_{10} determines the long-time relaxation of the correlation function. The corresponding eigenfunction (see, e.g., in [14]) reads

$$\psi_{10}(y, \dot{y}) = a (x - \tau_2 \dot{y}) \exp \left[-\frac{\dot{y}^2}{2\sigma_{\dot{y}\dot{y}}} - \frac{y^2}{2\sigma_{yy}} \right], \quad (47)$$

whereas the corresponding eigenfunction of the Hermitian adjoint operator reads

$$\psi_{10}^\dagger(y, \dot{y}) = y + \tau_2 \dot{y}. \quad (48)$$

The normalization determines the constant a ,

$$a = \frac{1}{2\pi D^2} \frac{\tau_1(\tau_1 + \tau_2)^2}{\tau_1 - \tau_2} \sqrt{\tau_1 \tau_1} \approx \frac{1}{2\pi D^2} \tau_1^2 \sqrt{\tau_1 \tau_2}. \quad (49)$$

At large times, the transition probability density is dominated by the spectral contribution of the smallest non-vanishing eigenvalue, i.e. [14],

$$P(y, \dot{y}, t | y', \dot{y}', 0) \approx p_2(y, \dot{y}) + \psi_{10}(y, \dot{y}) \psi_{10}^\dagger(y', \dot{y}', 0)$$

$$\times \exp \left[-\frac{1}{\tau_1} t \right]. \quad (50)$$

This in turn determines the long-time behavior of the correlation function (see, e.g., [14])

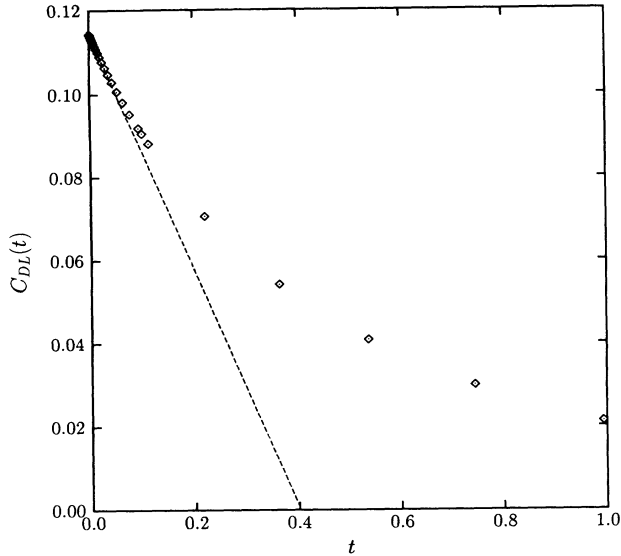


FIG. 2. The correlation function $C_{DL}(t)$ is shown for $\tau_1=0.9$, $\tau_2=0.1$, $d=0.2$, and $b=0.5$. The dashed line shows the short-time approximation (44). The squares show the numerical integration of (43).

$$C_{DL}(t) \approx \frac{1}{2\pi} \exp\left[-\frac{b^2}{\sigma_{yy}}\right] \exp\left[-\frac{1}{\tau_1}t\right], \quad (51)$$

i.e., a purely exponential decay. Note also here the different Arrhenius factors in the long-time behavior (51) and the short-time decay (44), which are similar to those in the single low-pass filtered process.

IV. TRIGGERED PROCESSES AND EXTERNAL SIGNALS

In this section, we consider a noisy threshold element driven by a periodic input signal. In terms of neuro-language, we add a periodic stimulus to the noisy neuron. For small external signals, i.e., smaller than the threshold, there would be no threshold crossing in the absence of noise. In the presence of noise, there will be noise induced threshold crossing, but at preferred instants of time, i.e., when the signal is larger. Although this mechanism looks similar to the synchronization of hopping in a bistable potential due to stochastic resonance, there are some significant differences. In symmetric bistable systems, driven by a weak periodic signal plus noise, there is a maximum of the response to the periodic signal when the period of the signal approximately matches twice the mean first passage time, leaving a basin of attraction. This matching condition implies a strong dependence of the optimal value of the noise on the driving frequency, i.e., the optimal value shifts towards zero for decreasing driving frequencies. In the presently discussed threshold-crossing dynamics, this optimal value of the noise strength does not depend on the driving frequency.

The stimulus $A \sin(\Omega t + \varphi)$ is taken into account in the SL and DL models by *adding* it to the noise. The corresponding probability density approaches for larger times the steady-state periodic function [15]

$$p_1(x, t) = \left[\frac{1}{2\pi\sigma} \right]^{1/2} \exp\left[-\frac{[x - A \sin(\Omega t + \varphi)]^2}{2\sigma} \right], \quad (52)$$

where the variance σ is given by $\sigma = D/\tau_1$.

For the double low-pass filtered process $y(t)$, the asymptotic steady-state distribution function for y and \dot{y} is given by [15]

$$p_2(y, \dot{y}, t) = \frac{1}{2\pi\sqrt{\sigma_{yy}\sigma_{\dot{y}\dot{y}}}} \exp\left[-\frac{[y - A \sin(\Omega t + \varphi)]^2}{2\sigma_{yy}} \right] \times \exp\left[-\frac{[\dot{y} - A \Omega \cos(\Omega t + \varphi)]^2}{2\sigma_{\dot{y}\dot{y}}} \right], \quad (53)$$

where the variances σ_{yy} and $\sigma_{\dot{y}\dot{y}}$ are given in (21).

A. Probability density

The steady-state probability density of the random pulse, given in (19), is obtained by taking the averages (22) with the asymptotic probability density (53), yielding for the DL model

$$p_0(t) = 1 - p_1(t),$$

$$p_1(t) = \frac{1}{\sqrt{2\pi\sigma_{yy}}} \int_b^\infty \exp\left[-\frac{[y - A \sin(\Omega t + \varphi)]^2}{2\sigma_{yy}} \right] dy = \frac{1}{2} \operatorname{erfc}\left[\frac{b - A \sin(\Omega t + \varphi)}{\sqrt{2\sigma_{yy}}} \right]. \quad (54)$$

The time dependence reflects the pacemaker function of the periodic stimulus for the noise induced threshold crossing. The probabilities are again not of Boltzmann type. For the SL model, σ_{yy} has to be substituted by $\sigma = D/\tau_1$.

B. Correlation of the random pulse with the signal

We now consider the correlation of the random pulse train with the external signal $A \sin(\Omega t)$ in time,

$$\begin{aligned} \kappa &= \langle\langle s_\Theta(t) \sin(\Omega t) \rangle\rangle_t \\ &= \frac{1}{2\pi/\Omega} \int_0^{2\pi/\Omega} dt \int_{-\infty}^\infty d\dot{y} \int_b^\infty dy p_2(y, \dot{y}, t) \sin(\Omega t). \end{aligned} \quad (55)$$

To further evaluate the integrals, we expand the exponentials in $p_2(y, \dot{y}, t)$ in a Fourier series according to

$$\begin{aligned} \exp(c \cos 2\theta) &= I_0(c) + 2 \sum_{k=1}^{\infty} I_k(c) \cos 2k\theta, \\ \exp(c \sin \theta) &= I_0(c) + 2 \sum_{k=0}^{\infty} (-1)^k I_{2k+1}(c) \sin(2k+1)\theta \\ &\quad + 2 \sum_{k=1}^{\infty} (-1)^k I_{2k}(c) \cos 2k\theta, \end{aligned} \quad (56)$$

where $I_n(c)$ denote Bessel functions with complex valued arguments [13]. Inserting this expansion into (55), we find the expression

$$\kappa = \frac{1}{\sqrt{2\pi\sigma_{yy}}} \exp\left[-\frac{A^2}{4\sigma_{yy}}\right] \left\{ I_0\left[\frac{A^2}{4\sigma_{yy}}\right] \int_b^\infty \exp\left[-\frac{y^2}{2\sigma_{yy}}\right] I_1\left[\frac{Ay}{\sigma_{yy}}\right] dy \right. \\ \left. + 2 \sum_{k=1}^\infty (-1)^k I_k\left[\frac{A^2}{4\sigma_{yy}}\right] \int_b^\infty \exp\left[-\frac{y^2}{2\sigma_{yy}}\right] I'_{2k}\left[\frac{Ay}{\sigma_{yy}}\right] \right\}. \quad (57)$$

For SL, we have to substitute σ_{yy} by $\sigma = D/\tau_1$. Generally, this integral is subject to numerical integration, but can be approximated for $\sigma_{yy} \gg A^2$ by expanding the Bessel functions for small arguments. In leading order of the modulation strength A , we find

$$\kappa = \frac{A}{2\sqrt{2\pi\sigma_{yy}}} \exp\left[-\frac{b^2}{2\sigma_{yy}}\right], \quad (58)$$

which shows a bell-shaped curve as a function of the variance σ_{yy} with a maximum at $\sigma_{yy}^{\max} = b^2$. The condition for the maximum does not involve the frequency of the signal, i.e., it is nondynamical. In Fig. 3, we show the square of the correlation κ for various values of the signal strength. Although the signal is smaller than the threshold, the threshold element transfers the signal to the output via synchronized noisy firing (see also [4]). When the signal strength becomes larger than the threshold, i.e., the threshold crossing is mainly due to the signal, the maximum disappears and we find a monotonous decreasing correlation as a function of the variance.

The decay of the correlation κ for larger variance is proportional to the inverse of the square root of the variance. This decay is slower than in the corresponding curves in the case of symmetric two-state systems, where one observes a decay proportional to the inverse variance. Assuming uncorrelated threshold-crossing events (Poisson statistics), the recent analysis by Wiesenfeld *et al.* [3]

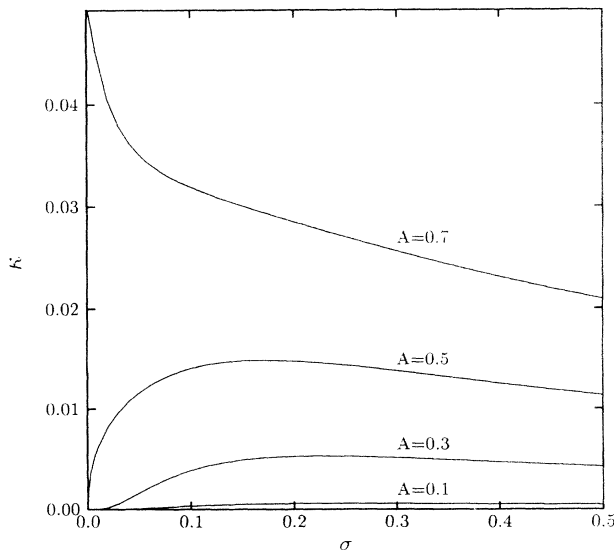


FIG. 3. The correlation κ (57) is shown at $b = 0.5$ as a function of the variance at different values of the signal strength. For DL, σ is given by $\sigma_{yy} = D/(\tau_1 + \tau_2)$, while for SL, $\sigma = D/\tau_1$.

yields, as for two-state dynamics, a decay of $\kappa \propto \sigma^{-4}$. In Fig. 4, we show the input-output characteristic of the threshold device for several noise levels. For vanishing noise, the correlation κ is obtained by taking the average over the uniformly distributed phase and a δ -shaped probability, i.e.,

$$p_2(y, \dot{y}) = \delta(y - A \sin(\Omega t + \varphi)) \delta(\dot{y} - A \Omega \cos(\Omega t + \varphi)), \quad (59) \\ \kappa = \frac{1}{2\pi} \int_0^{2\pi} d\varphi \int_b^\infty dy \delta(y - A \sin(\varphi)) \sin(\varphi) \\ = \frac{1}{A\pi} \sqrt{A^2 - b^2}.$$

Above threshold, i.e., $A > b$, noise reduces the output, whereas below threshold noise—up to a certain level—upgrades the output.

This mechanism has possible technological applications, since all logical functions (AND, OR, NAND, . . .), which are important for digital electronics, can be constructed out of threshold elements (see, e.g., [16]). In particular, nanoscale devices which have typically a gain of two orders less than conventional devices are suffering from large scattering with respect to their electrical prop-

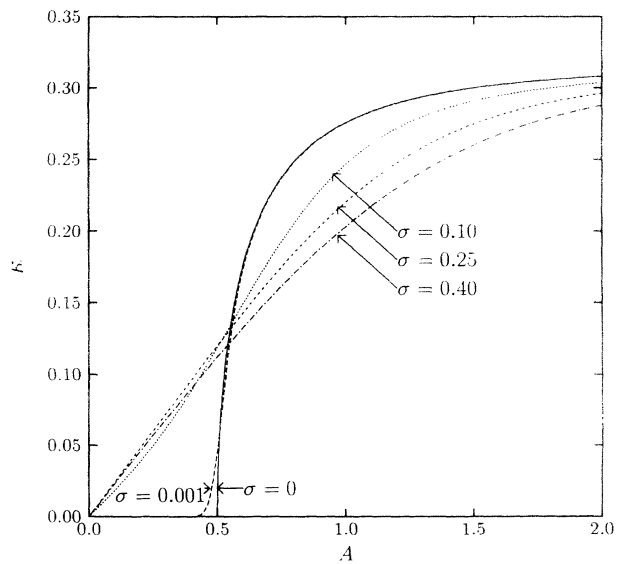


FIG. 4. The correlation κ (57) is shown at $b = 0.5$ as a function of the amplitude A of the modulation at various values of the variance σ . The curve for $\sigma = b^2 = 0.25$ represents an upper limit below threshold. For DL, σ is given by $\sigma_{yy} = D/(\tau_1 + \tau_2)$, while for SL, $\sigma = D/\tau_1$.

erties. The reliability of such devices is still not sufficient in order that they could be used for building devices for computing. Other concepts, such as highly redundant neuronal computing strategies, are currently under investigation. Within this concept, the role of fluctuations with respect to subthreshold signal processing as a useful tool might be viewed from a different perspective.

The quality of a signal corrupted by noise is described in the engineering community by a signal-over-noise ratio (SNR). In this paper, we consider the SNR for small external signals as the square of the correlation coefficient κ and the spectral density of the unstimulated pulse train at the frequency of the external signal. This definition is completely equivalent to taking the ratio of the weight of the δ spike in the power spectrum and the noise background at the same frequency (for a discussion, see [15]) as long as the external signal is small. Although in our theory there is no restriction to small driving frequencies, we have computed the SNR in this regime. Since the signal part shows in leading order a trivial dependence on A^2 , we further have divided the SNR (R_{SN}) by this quantity, yielding

$$(R_{SN}) = \frac{\kappa^2}{A^2 S(\omega=0)} = \frac{\kappa^2}{A^2 \int_0^\infty C_{SL(DL)}(t) dt}. \quad (60)$$

In Fig. 5, the signal-over-noise ratio for the single low-pass filtered case is shown for $\tau_1=1$ and $b=0.5$ as a function of the variance. The curve also shows a peak, which is shifted towards smaller values of the variance in comparison to the peak in the correlation κ . In Ref. [5], the SNR in contrast does not show a peak, indicating a loss of coherence due to dephasing at every event. The static condition for the maximum $\sigma_{yy}^{\max}=b^2$ does not hold, an indication that the more natural quantity describing this effect is rather the correlation coefficient κ . It is interest-

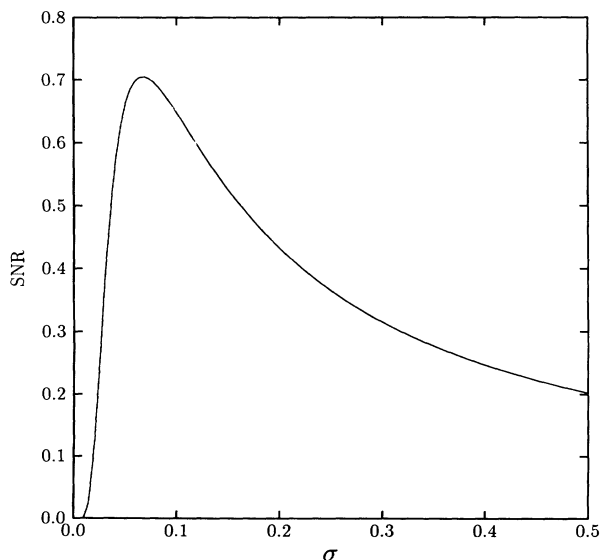


FIG. 5. The signal-over-noise ratio (60) is shown for SL as a function of the variance $\sigma = D/\tau_1$ at $b=0.5$.

ing to note that while the noise decreases with increasing frequency, the signal does not depend on it.

V. CONCLUSIONS

We have discussed the statistical properties of random pulse trains generated by a noisy threshold-crossing element—a simple model for the firing of neurons. The correlation function of the random pulse train shows algebraic decay for small times, indicating the lack of a time scale. The power spectrum accordingly shows also algebraic decay at large frequencies. The algebraic decay of correlations in the case of a Markovian noise source is a manifestation of the fractal properties of the generated random pulse train. Additional low-pass filtering smoothens the process on short time scales, thereby destroying the statistical self-similarity.

We have further studied the impact of noise on the response of the threshold device on periodic signals. The role of noise for the signal transfer is ambiguous. In the absence of noise, the threshold device does not respond for signals less than the threshold. Above threshold, the device starts to respond and eventually saturates for large signal strength A . Below threshold, noise triggers signal transmission to the output. Starting at zero noise, the transmitted amplitude first increases with increasing noise strength until it reaches a maximum and then decreases again. Above threshold noise always decreases the transmitted signal amplitude. Recent experiments with mechanoreceptor cells of crayfishes [3] yield response curves as a function of the noise with a rising part for small noise, a maximum, and a decaying part for large noise. The theory presented in [3] accounts very well for the rising part and the maximum, but yields a too fast decay for large noise. A possible reason for the disagreement is the neglect of correlations between crossing events in [3]. Since crossings are more frequent for large fluctuations, one expects correlations to be important for large fluctuations. The analysis presented in this paper does not assume an underlying Poisson statistics and thus does not neglect correlations between threshold-crossing events. Although other phenomena such as refractory periods have been neglected here and in [3], the large noise decay of our results agrees better with the one observed in the experiments.

ACKNOWLEDGMENTS

This work has been stimulated by numerous discussions with Frank Moss. I wish to thank him and Laszlo Kiss also for making available to me their research results prior to publication. This work is financially supported by the Deutsche Forschungsgemeinschaft within the Heisenberg program.

APPENDIX

The transition probability density $P(x, t|x', 0)$ is expanded into the complete set of eigenfunctions $\psi_n(x)$ of the Fokker-Planck operator,

$$\mathbf{L}_{\text{FP}} = \frac{1}{\tau_1} \frac{\partial}{\partial x} + \frac{D}{\tau_1^2} \frac{\partial^2}{\partial x^2}, \quad (\text{A1})$$

generating the stochastic process (6), i.e.,

$$\psi_n(x) = \frac{1}{\sqrt{2\pi\sigma 2^n n!}} H_n \left[\frac{x}{\sqrt{2\sigma}} \right] \exp \left[-\frac{x^2}{2\sigma} \right], \quad (\text{A2})$$

where $\sigma = D/\tau_1$. The corresponding eigenvalues are given by

$$\lambda_n = n \frac{1}{\tau_1}, \quad n = 0, 1, 2, \dots \quad (\text{A3})$$

The stationary correlation function $C(t)$ is then written in terms of the eigenfunctions and eigenvalues

$$\begin{aligned} C(t) &= \langle s_\Theta(t) s_\Theta(0) \rangle - \langle s_\Theta \rangle^2 \\ &= \sum_{n=1}^{\infty} \exp(-\lambda_n t) \int_b^{\infty} \psi_n(x) dx \int_b^{\infty} dx' \psi_n^\dagger(x') \psi_0(x'), \end{aligned} \quad (\text{A4})$$

where $\psi_n^\dagger(x')$ are the eigenfunctions of the Hermitian adjoint operator $\mathbf{L}_{\text{FP}}^\dagger$, given by

$$\psi_n^\dagger(x') = \frac{1}{\sqrt{2^n n!}} H_n \left[\frac{x'}{\sqrt{2\sigma}} \right]. \quad (\text{A5})$$

Using the relation [13]

$$\begin{aligned} \int_b^{\infty} dx H_n \left[\frac{x}{\sqrt{2\sigma}} \right] \exp \left[-\frac{x^2}{2\sigma} \right] \\ = \sqrt{2\sigma} H_{n-1} \left[b \frac{1}{\sqrt{2\sigma}} \right] \exp \left[-\frac{b^2}{2\sigma} \right] \end{aligned} \quad (\text{A6})$$

we find for the correlation function

$$C(t) = \frac{1}{2\pi} \exp \left[-\frac{b^2}{2\sigma} \right] \sum_{n=1}^{\infty} \exp \left[-\frac{nt}{\tau_1} \right] \frac{H_{n-1}^2(b/\sqrt{2\sigma})}{2^n n!}. \quad (\text{A7})$$

For large times, the main contribution stems from the smallest nonvanishing eigenvalue $\lambda_{\min} = 1/\tau_1$, yielding

$$C(t) = \frac{1}{2\pi} \exp \left[-\frac{b^2}{2\sigma} - \frac{t}{\tau_1} \right]. \quad (\text{A8})$$

Taking the derivative of the correlation function with respect to time, rearranging the sum, and using Mehler's formula, i.e.,

$$\begin{aligned} \sum_{n=0}^{\infty} \frac{1}{2^m m!} \exp \left[-m \frac{t}{\tau_1} \right] H_m^2(x) \\ = \frac{\exp \left\{ x^2 \left[1 - \frac{[1 - \exp(-t/\tau_1)]^2}{1 - \exp(-2t/\tau_1)} \right] \right\}}{\sqrt{1 - \exp(-2t/\tau_1)}}. \end{aligned} \quad (\text{A9})$$

we arrive at the closed expression for the derivative of the correlation function,

$$\begin{aligned} \dot{C}(t) &= -\frac{1}{2\pi\tau_1} \exp \left[-\frac{t}{\tau_1} \right] \frac{\exp(-b^2/2\sigma)}{\sqrt{1 - \exp(-2t/\tau_1)}} \\ &\times \exp \left[-\frac{b^2}{2\sigma} \frac{[1 - \exp(-t/\tau_1)]^2}{1 - \exp(-2t/\tau_1)} \right]. \end{aligned} \quad (\text{A10})$$

Both limits, the limits for small and large times, can be readily reobtained from (A10).

- [1] (a) A. L. Hodgkin and A. F. Huxley, *J. Physiol.* **117**, 500 (1952); (b) R. Fitzhugh, *Biophys. J.* **1**, 445 (1961); (c) S. Nagumo, S. Arimoto, and S. Yoshizawa, *Proc. IRE* **50**, 2061 (1962).
 [2] W. S. McCulloch and W. Pitts, *Bull. Math. Biophys.* **5**, 115 (1943).
 [3] K. Wiesenfeld, D. Pierson, E. Pantazelou, C. Dames, and F. Moss, *Phys. Rev. Lett.* **72**, 2125 (1994).
 [4] R. Fox, R. Roy, and G. Vemuri (unpublished).
 [5] A. Bulsara and S. Lowen, *Phys. Rev. E* **49**, 4989 (1994).
 [6] S. B. Loewen and M. C. Teich, *Phys. Rev. E* **47**, 992 (1993).
 [7] Z. Gingl, L. B. Kiss, and F. Moss (unpublished).
 [8] P. Hanggi, P. Talkner, and M. Borkovec, *Rev. Mod. Phys.* **62**, 251 (1990).
 [9] S. O. Rice, in *Noise and Stochastic Processes*, edited by N.

- Wax (Dover, New York, 1954), p. 133.
 [10] R. L. Stratonovich, *Theory of Random Noise* (Gordon and Breach, New York, 1967), Vol. II.
 [11] H. A. Kramers, *Physica* **7**, 284 (1940).
 [12] J. Hertz, A. Krogh, and R. G. Palmer, *Introduction to The Theory of Neural Computing*, Lecture Notes Vol. 1, Santa Fe Institute Studies in the Science of Complexity (Addison-Wesley, Reading, MA, 1991).
 [13] *Handbook of Mathematical Functions*, edited by M. Abramowitz and I. Stegun (Dover, New York, 1964).
 [14] H. Risken, *The Fokker-Planck Equation*, Springer Series in Synergetics Vol. 18 (Springer-Verlag, Berlin, 1984).
 [15] P. Jung, *Phys. Rep.* **234**, 175 (1993).
 [16] M. L. Minsky, *Computation: Finite and Infinite Machines*, (Prentice-Hall, Englewood Cliffs, NJ, 1967).